Contents lists available at ScienceDirect

Surface Science

First-principles calculations of the thermal stability of Ti$_3$SiC$_2$(0001) surfaces

Walter Orellana [a], Gonzalo Gutiérrez [b],*

[a] *Departamento de Ciencias Físicas, Universidad Andres Bello, Av. República 220, 837–0134, Santiago, Chile*
[b] *Departamento de Física, Facultad de Ciencias, Universidad de Chile, Casilla 653, Santiago, Chile*

ABSTRACT

The energetic, thermal stability and dynamical properties of the ternary layered ceramic Ti$_3$SiC$_2$(0001) surface are addressed by density-functional theory calculations and molecular dynamic (MD) simulations. The equilibrium surface energy at 0 K of all terminations is contrasted with thermal stability at high temperatures, which are investigated by *ab initio* MD simulations in the range of 800 to 1400 °C. We find that the toplayer (sublayer) surface configurations: Si(Ti2) and Ti2(Si) show the lowest surface energies with reconstruction features for Si(Ti2). However, at high temperatures they are unstable, forming disordered structures. On the contrary, Ti1(C) and Ti2(C) despite their higher surface energies, show a remarkable thermal stability at high temperatures preserving the crystalline structures up to 1400 °C. The less stable surfaces are those terminated in C atoms, C(Ti1) and C(Ti2), which at high temperatures show surface dissociation forming amorphous TiC$_x$ structures. Two possible atomic scale mechanisms involved in the thermal stability of Ti$_3$SiC$_2$(0001) are discussed.

© 2011 Elsevier B.V. All rights reserved.

1. Introduction

The layered ternary compound Ti$_3$SiC$_2$ is a representative member of the M$_{n+1}$AX$_n$ class of materials, known as MAX phases, which are increasingly important due to their remarkable combination of properties between metals and ceramics (e.g. stiff, lightweight and ductile) [1–3]. The resistance to thermal shock, oxidation and damage is additional properties reported, [4–7] suggesting applications for this material as high-temperature oxidation and thermal barrier coatings.

The high-temperature stability of Ti$_3$SiC$_2$ in bulk and thin films is rather controversial. Early reports show that sintered Ti$_3$SiC$_2$ is thermally stable up to at least 1700 °C, [2,8] and possibly up to 2300 °C [9]. However, it has been reported that approximately at 1450 °C, Ti$_3$SiC$_2$ shows a stress anomaly, [10] which has been attributed to a structural transition from α- to β-Ti$_3$SiC$_2$ that would take place at about 1270 °C, according to molecular dynamic simulations [11]. Other groups have reported that the bulk phase becomes unstable at temperatures higher than 1400 °C in an inert atmosphere (e.g., vacuum, argon, or nitrogen) [12–14]. More recent experiments have shown that Ti$_3$SiC$_2$ is susceptible to thermal dissociation during annealing from 1200 °C in vacuum or low oxygen partial pressure, forming porous surface coating of TiC$_x$ and Ti$_5$Si$_3$C$_x$ [15]. On the other hand, studies of phase decomposition in epitaxial Ti$_3$SiC$_2$ (0001) indicate that thin films are effectively stable during vacuum annealing up to 1000–1200 °C, above which a decomposition is initiated by out-diffusion and evaporation of Si atoms from the top (0001) surface on a nanometer depth scale [16,17]. The difference in the observed decomposition temperature between bulk and thin-films Ti$_3$SiC$_2$ has been attributed to diffusion length scales and measurement sensitivity. However, the fundamental knowledge of the thermal stability in Ti$_3$SiC$_2$(0001) films is limited and decomposition processes at atomic scale are poorly understood. The inverse process has also been investigated, that is, the solid-state synthesis of MAX phases, particularly Ti$_3$AlC$_2$, by considering the rapid intercalation of Al atoms in TiC$_x$ (x<1), or TiC compounds with C-vacancy ordering [18]. Theoretical results have shown low difference in energy between the C vacancy and the Al substitution at the vacant C site, of about 0.2 eV, [19] suggesting that the intercalation mechanism would be likely to occur driven by temperature. A similar result should be expected for the intercalation of Si atoms due to their high mobility [20].

The surface stability and equilibrium geometry (at 0 K) of Ti$_3$SiC$_2$ (0001) have been theoretically investigated by *ab initio* calculations, considering the minimal (1×1) surface periodicity [21,22]. In those works, the most stable terminations were obtained by comparing their surface energies γ [Eq. (1)], where lower values of γ indicate more stable surfaces. These calculations showed that the titanium terminations would be the most stable surfaces while those terminated in carbon the less stable, with a difference in surface energy of about 5 J/m^2. Surface energetics using the same theoretical approach have reported similar results for other M$_{n+1}$AX$_n$ materials [23,24]. However, reconstructions are common features of surfaces which cannot be addressed by the minimal surface periodicity. In addition, kinetic and dynamic effects are not previously investigated from a theoretical point of view.

* Corresponding author. Tel.: +56 2 9787283.
E-mail addresses: worellana@unab.cl (W. Orellana),
gonzalo@fisica.ciencias.uchile.cl (G. Gutiérrez).

In this work we study the equilibrium structure and energetic of Ti$_3$SiC$_2$(0001) in all their terminations, using both (1×1) and (3×3) surface periodicity. We also investigate the evolution of the Ti$_3$SiC$_2$ (0001) − (3×3) terminations at high temperatures by *ab initio* molecular dynamic (MD) simulations. Our results reveal interesting features like reconstructions at 0 K on Si- and C-terminated surfaces, showing lower surface energies than those previously reported in the literature. At high temperatures, the most stable surfaces are those terminated in Ti atoms follow by C atoms, which preserve the crystalline structures up to 1400 °C. Other terminations show instabilities associated to the formation of Si-Si and C-C bonds, inducing toplayer disorder and amorphization in close agreement with experimental results [16].

2. Theoretical method

The calculations were carried out in the framework of density functional theory, within the generalized gradient approximation to the exchange and correlation potential [25]. We use a basis set of localized atomic orbitals (double-ζ plus polarization functions, DZP), and norm-conserving pseudopotentials as implemented in the *ab initio* simulation package SIESTA [26]. Ti$_3$SiC$_2$ crystallizes in a hexagonal structure (space group $P6_3/mmc$), growing commonly along the (0001) direction. Our calculated lattice parameters are found to be of $a = 3.08$ Å and $c = 17.71$ Å, in good agreement with experimental results ($a = 3.068$ Å and $c = 17.669$ Å), [1] and plane-wave calculations [11]. The Ti$_3$SiC$_2$ structure shows two inequivalent Ti atoms, usually referred in the literature as Ti1 and Ti2, where Ti1 occupies the (0, 0, z) position (Wyckoff position 2a) and Ti2 the (1/3, 1/3, z) or (2/3, 2/3, z) positions (Wyckoff position 4f). Thus, two bonding structures for titanium are formed, C-Ti1-C and C-Ti2-Si, resulting in six different terminations along (0001) direction which are denoted: C(Ti1), C(Ti2), Si(Ti2), Ti1(C), Ti2(C), and Ti2(Si); in parenthesis are indicated the subsurface atomic layer. The stability of the surfaces is studied by the symmetrical slab method considering (1×1) and (3×3) surface unit cells with the same number of monolayers (MLs), ranging from 19 to 23, and a vacuum region of 15 Å. The atomic relaxation is performed for the first 8 MLs at both ends of the slab until the force component at each atom becomes smaller than 0.05 eV/Å. The Brillouin zone (BZ) sampling is performed with a 3×3×1 Monkhorst–Pack mesh. As a test of convergence for our basis we calculate the cohesive energy of bulk Ti$_3$SiC$_2$ considering a larger basis set (triple-ζ plus polarization functions, TZP). We find a cohesive energy of 6.05 eV (6.19 eV) using DZP (TZP), showing that our choice of a DZP basis set gives reasonably converged results.

The surface energy of the symmetrical-terminated slab at zero temperature and negligible pressure is given by $\gamma = (E_t - \sum n_i \mu_i)/2A$, where E_t and A are the total energy and the slab area, respectively. Whereas, n_i and μ_i are the number of atoms and chemical potentials of the atomic species ($I = $ Ti, Si, C). The chemical potentials are constrained to vary according to the stoichiometric relation $\mu_{Ti_3SiC_2} = 3\mu_{Ti} + \mu_{Si} + 2\mu_C$. Thus, combining the aforementioned equations and taking μ as the energy per atom of the respective bulk phases, the surface energy can be calculated by

$$\gamma = \frac{1}{2A}\left[E_t - \left(\frac{n_C}{2}\right)\mu_{Ti_3SiC_2} - \left(n_{Ti} - \frac{3}{2}n_C\right)\mu_{Ti} - \left(n_{Si} - \frac{n_C}{2}\right)\mu_{Si}\right]. \quad (1)$$

The surface stability at high temperature is studied by *ab initio* MD simulations at constant temperature, using the Nosé-thermostat approach [27]. In this formalism, the system is in thermal contact with a heat bath, which can exchange energy in order to fix the system temperature, simulating a canonical ensemble. The dynamical properties of the different terminations are investigated at 800, 1000, 1200, and 1400 °C during 4 ps, considering 1 ps for each temperature. The time step is chosen to be of 1 fs. For these calculations we use

nonsymmetrical (3×3) surface unit cells with 8 and 9 MLs, where the bottommost two MLs are fixed in their equilibrium bulk geometry. For the BZ sampling we use the Γ point.

3. Results and discussion

Table 1 shows our results for the surface and relaxation energies of Ti$_3$SiC$_2$(0001) calculated with a (3×3) surface periodicity in all their terminations. Here, we also include our results for the minimal (1×1) periodicity. The relaxation energy can give us a measure of toplayer bond strength. It is calculated with the symmetrical slabs by taken half the value of the energy difference between the relaxed and unrelaxed structures. We find large relaxation energies for C(Ti1) of 17 eV as well as for C(Ti2) and Si(Ti2) of 3 eV, indicating surface reconstructions which are not observed in the minimal surface unit cell. The surface energy is calculated from Eq. (1). We find that Si(Ti2), Ti2(Si) and Ti1(C) are energetically more stable with surface energies of 1.82, 1.88, and 2.53 J/m^2, respectively. While C(Ti1) and C(Ti2) would be less stable because their large surface energies of 8.49 and 8.45 J/m^2. Using the minimal surface unit cell we find similar results, excepting for C(Ti1) and Si(Ti2) which exhibit higher surface energies by about 3.3 and 0.8 J/m^2, respectively. Thus, calculations with the minimal surface unit cell indicate less stable terminations for C(Ti1) and Si(Ti2) which is another evidence for their in-plane reconstructions.

Fig. 1(a)–(c) shows equilibrium geometries (at 0 K) for the lower surface-energy terminations: Si(Ti2), Ti2(Si) and Ti1(C), respectively. We find that Si(Ti2) does not preserve its hexagonal symmetry, forming Si-Si bonds that result in a disordered structure. This is reflected in a large surface relaxation energy of about 3 eV. The distance between Si and Ti layers increases by 10% with respect to the bulk Ti$_3$SiC$_2$. The average Si–Si bond distance of the disordered Si toplayer is found to be of 2.56 Å. This reconstruction leaves clearances that expose the subsurface Ti layer, depicted in yellow in Fig. 1(a). For the Ti2(Si) and Ti1(C) terminations we find equilibrium geometries that preserve the symmetry, that is without reconstructions, as shown Fig. 1(b) and (c). The Ti2(Si) termination maintains almost unchanged the Ti–Si interplanar distance when compared with bulk Ti$_3$SiC$_2$, whereas for the Ti1(C) termination the Ti–C interplanar distance is shorter by 17%. From these results we can infer that the Ti–Si bonds are much weaker than the Ti–C bonds, which agree with experimental results in bulk Ti$_3$SiC$_2$ [20].

Fig. 1(d)–(f) shows snapshots obtained from MD simulations at 1400 °C after 1 ps for Si(Ti2), Ti2(Si) and Ti1(C) terminations, respectively. These snapshot images give us an idea of the changes in the surface structures at high temperature. For Si(Ti2) the MD simulations show a high mobility of the topsurface Si atoms from 1000 °C, forming Si–Si bonds continually, whereas desorptions are observed from 1200 °C, in close agreement with experimental results [16,17]. Meanwhile, the subsurface Ti atoms vibrate around their positions keeping the structural geometry. For Ti2(Si) [Fig. 1(e)], we observe a strong thermal motion of the subsurface Si atoms with large amplitudes. This movement induces the formation of Si-Si bonds at the

Table 1
Calculated surface energy (γ) and relaxation energy (E_r) for all the Ti$_3$SiC$_2$(0001) terminations using the symmetrical slab method with 1×1 and 3×3 surface periodicity. Termination corresponds to topsurface and subsurface (in parenthesis) atomic layers.

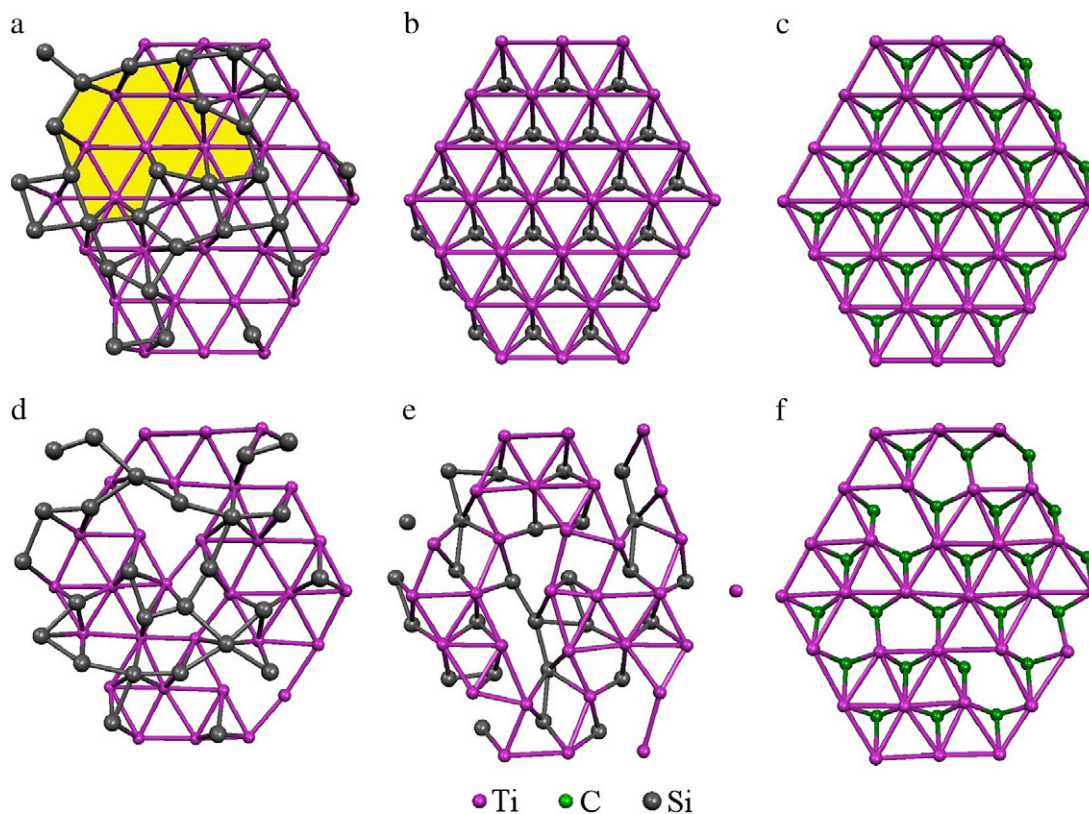| Termination	1×1		3×3	
	E_r(eV)	γ(J/m^2)	E_r(eV)	γ(J/m^2)
C(Ti1)	−0.47	11.82	−17.15	8.49
C(Ti2)	−0.84	8.59	−3.74	8.45
Si(Ti2)	−0.07	2.57	−3.27	1.82
Ti1(C)	−0.29	2.65	−0.10	2.53
Ti2(C)	−0.10	4.15	−0.02	3.98
Ti2(Si)	−0.08	1.96	−0.43	1.88

Fig. 1. (Color online) Topview of the first two monolayers of $Ti_3SiC_2(0001)$ in their lower surface energy terminations. (a)-(c) Equilibrium geometry at 0 K of Si(Ti2), Ti2(Si), and Ti1(C), respectively. (d)–(f) Snapshots of the MD simulation at 1400 °C for the same terminations.
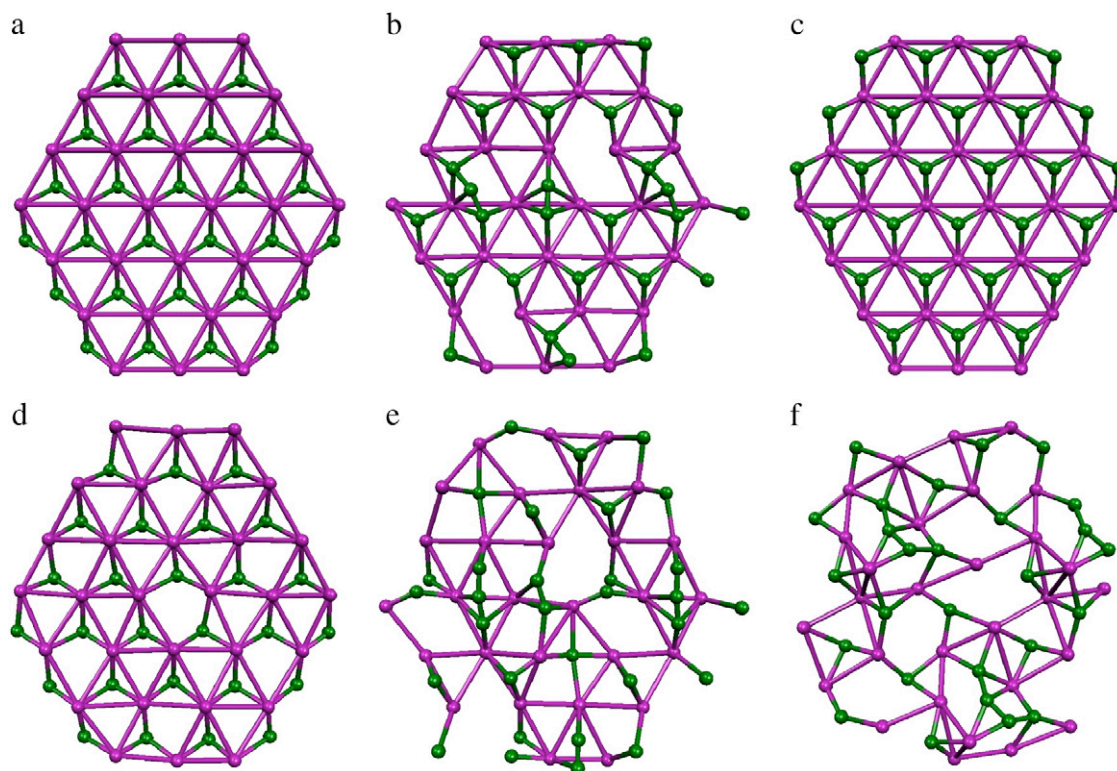

Fig. 2. (Color online) Topview of the first two monolayers of $Ti_3SiC_2(0001)$ in their higher surface energy terminations. (a)–(c) Equilibrium geometry at 0 K of Ti2(C), C(Ti1), and C(Ti2), respectively. (d)–(f) Snapshots of the MD simulation at 1400 °C for the same terminations.

subsurface during short periods of times, introducing an in-plane anisotropy and the disorder of the toplayer Ti atoms. It is worthy of note that anisotropic vibrations of the Si atoms with large amplitude in Ti_3SiC_2 have been recently observed by high-temperature neutron diffraction experiments [20,28]. In addition, the high mobility observed of the Si atoms at subsurface may support possible routes for MAX phases solid-state synthesis recently suggested in Ti_3AlSi_2 [18,19]. The most interesting case occurs for Ti1(C). This termination shows a high stability with temperature, preserving its structure up to 1400 °C, as shown the MD simulation snapshots of Fig. 1(f). In short, the weakness of the Si–Ti bond, as compared with the C–Ti bond provokes strong Si thermal motions with large amplitude, inducing topsurface disorder when the Si layer is close to the surface. For Ti2(Si), the Si layer is located in the second sublayer, accordingly this termination exhibits a high mobility with temperature which is not observed in Ti1(C) where the Si layer is located at the fourth sublayer.

Fig. 2(a)–(c) shows equilibrium geometries (at 0 K) for the higher surface-energy terminations: Ti2(C), C(Ti1) and C(Ti2), respectively. The Ti2(C) termination does not show reconstructions, just an interplanar reduction between Ti and C layers of about 11% with respect to the bulk structure. C(Ti2) also preserves its structure but with a stronger relaxation, reducing the distance between C and Ti layers by 43%. Accordingly, the relaxation energy of the Ti2(C) and C(Ti2) terminations is found to be of 0.02 and 3.7 eV, respectively. For C(Ti1) we find the largest relaxation energy among all terminations, of about 17 eV. This strong relaxation is associated to the formation of toplayer C-C bonds, which are energetically much more favorable than the toplayer C–Ti bonds [Fig. 2(b)]. We observe two new geometries for the C atoms: (i) a linear C trimer with bond distance of 1.36 Å and C–C–C angle of about 150°, and (ii) a C dimer with bond distance of 1.32 Å. The C–C bond length in the above configurations suggests a double bond for the C atoms, as compared with ethylene (1.34 Å).

Fig. 2(d)–(f) shows snapshots obtained from MD simulations at 1400 °C after 1 ps for Ti2(C), C(Ti1) and C(Ti2) terminations, respectively. Our results show that Ti2(C) exhibits a high stability, preserving its structure along the range of temperature studied. In this termination, the Si layer is located far from the surface, in the sixth sublayer. A similar high stability is observed for Ti1(C) where the Si layer is located in the fourth sublayer. According to the aforementioned results, the surface stability of Ti-terminated surfaces might be associated with the depth of the Si layer. For C(Ti1) we observe a

high mobility of the C atoms, forming topsurface dimers and diffusing to the third C layer forming another dimers. This C diffusion produces an amorphous topsurface TiC_x structure which is observed from 800 °C. For this termination, the Si layer is located far in the fifth sublayer so that the amorphization can be associated entirely with the C diffusion. Finally, for the C(Ti2) termination the two topmost layers also tend to form an amorphous TiC_x structure weakly bonded to the third Si layer, driving by the C diffusion. This TiC_x structure takes an almost planar shape which begins to desorb from the Si layer at 1400 °C. The C–C bond formation has been observed by photoemission studies in $Ti_3SiC_2(0001)$ after annealing at 1000 °C [16]. Assuming that $Ti_3SiC_2(0001)$ is not naturally C terminated, the authors suggest that the observed C–C bonding would have a foreign origin. According to our results, C-terminated surfaces are energetically unlikely, however the C–C bonding in C-terminated $Ti_3SiC_2(0001)$ is likely to form and would explain the experimental data. Thus, we believe that the presence of C terminations is possible at high temperature and might originate in the C diffusion to surface defects or steps.

More detailed analysis regarding the changes of the toplayer structures with temperature can be done by plotting pair distribution functions $g(r)$. Fig. 3 shows the $g(r)$ for the first two monolayers of the surfaces whose terminations are composed by Si and Ti atoms, and Fig. 4 for those surfaces with terminations composed by C and Ti atoms. Fig. 3(a) and (b) shows the $g(r)$ for Si(Ti2) and Ti2(Si),
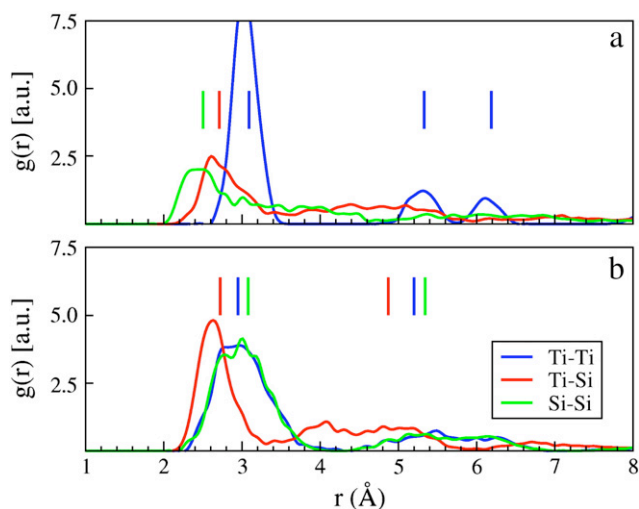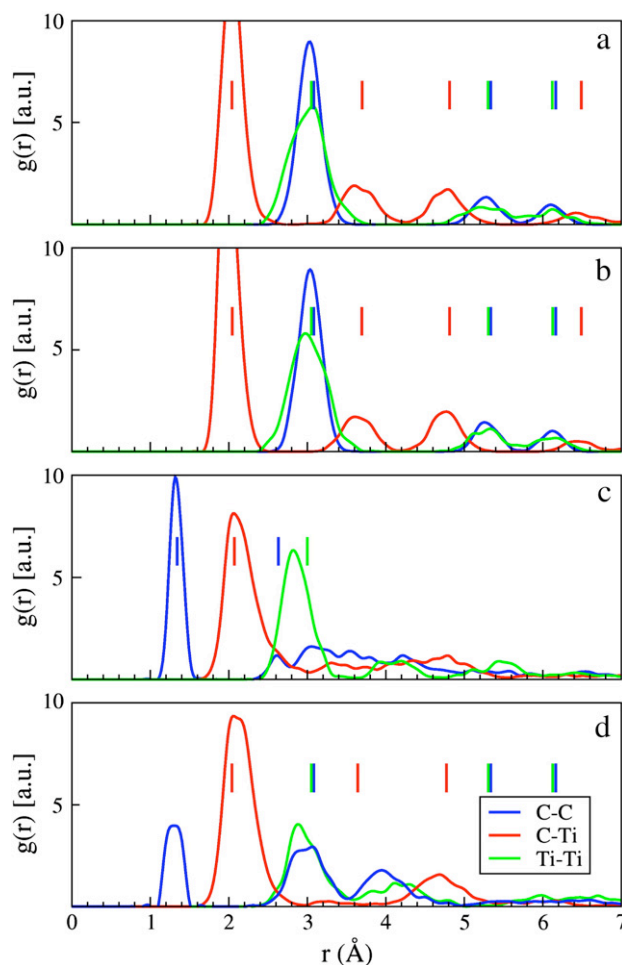
Fig. 4. (Color online) Pair distribution function for the first two monolayers of $Ti_3SiC_2(0001)$ at 1400 °C. (a) Ti1(C), (b) Ti2(C), (c) C(Ti1), and (d) C(Ti2). Vertical lines indicate pair distances for the surface geometries at 0 K.

Fig. 3. (Color online) Pair distribution function for the first two monolayers of Ti_3SiC_2 (0001) at 1400 °C. (a) Si(Ti2) and (b) Ti2(Si). Vertical lines indicate pair distances for the surface geometries at 0 K.

respectively, resulting from the MD simulation at 1400 °C. As can be seen in Fig. 3(a), the Si–Si distribution displays a wide first peak with a flat tail, indicating that the surface Si atoms have a liquid-like behavior. Note that the first peak is centered around 2.5 Å, in close agreement with experimental results of the liquid Si phase [29]. On the other hand, the Ti–Ti distribution displays well-defined peaks centered around the crystalline pair distances, indicating that the subsurface Ti atoms preserve their crystalline structure. For the case of Ti–Si, its distribution follows a similar trend as Si–Si which is consistent with the toplayer disorder. For Ti2(Si) we observe that the Si–Si and Ti–Ti distributions are almost the same, displaying a single wide peak around 3 Å with a flat tail, indicating that both Ti and Si layers are disordered. In fact, the topsurface Ti atoms follow the strong movement of the subsurface Si atoms, as shown in our simulations.

Fig. 4(a)–(d) shows the $g(r)$ for Ti1(C), Ti2(C), C(Ti1), and C(Ti2), respectively. For Ti1(C) and Ti2(C) we observe very similar pair distributions with well-defined peaks for C–C, C–Ti and to a lesser extend for Ti–Ti, all centered around the crystalline pair distances. This is a clear indication of the high stability of the Ti-terminated surfaces. In contrast, for C(Ti1) we find a thin C–C peak around 1.3 Å which corresponds to the C–C bonds formed at 0 K after the reconstruction. The absence of additional peaks indicates the structure amorphization. For C(Ti2), the C–C distribution also shows the C–C bond formation which in this case is induced by the temperature. The C–C bonds originated in the toplayer C atoms that diffuse both in-plane and downward to the third C monolayer. Another peak is found around 4 Å which is not present in the crystalline structure, showing that the amorphization is induced by the C diffusion.

4. Summary and conclusions

Using *ab initio* calculations we have studied the energetic, structural and dynamical properties of $Ti_3SiC_2(0001) - (3 \times 3)$ in all their terminations. We find that Si(Ti2) and Ti2(Si) show the lower surface energies, indicating the most stable terminations at 0 K. Si(Ti2) also exhibits toplayer reconstruction forming Si–Si bonds. However, at high temperatures >1200 °C, the Si(Ti2) termination is unstable, showing a liquid-like behavior and desorptions. Whereas Ti2(Si) shows a high mobility induced by the thermal motion of the subsurface Si atoms but preserving the crystalline structure. For C(Ti1) and C(Ti2) we found the highest surface energies indicating the less stable surfaces. C(Ti1) shows surface reconstructions, forming toplayer C-C bonds. At high temperatures the diffusion of C atoms increases the C–C bond formation, inducing the formation of a topsurface amorphous TiC_x structure. The most interesting results are found for Ti1(C) and Ti2(C) terminations, although with higher surface energies, these surfaces show a remarkable thermal stability at high temperatures

preserving the crystalline structures up to 1400 °C. The above results suggest that the surface instability of $Ti_3SiC_2(0001)$ with temperatures might be associated with two mechanisms: (i) the C diffusion and subsequent C–C bond formation for the C(Ti1) and C(Ti2) terminations, and (ii) the strong thermal motion of the Si layer and its proximity to the topsurface for the case of the Si(Ti) and Ti(Si) terminations. Here, the weakness of the Si–Ti bonds as compared with the C–Ti bonds provokes a high Si mobility with temperature inducing toplayer liquid-like disorder due to the continuous formation of Si–Si bonds.

References

[1] W. Jeitschko, H. Nowotny, F. Benesovsky, Montash. fur Chem. 98 (1967) 329.
[2] M.W. Barsoum, Prog. Sol. St. Chem. 28 (2000) 201.
[3] H.B. Zhang, Y.W. Bao, Y.C. Zhou, J. Mater. Sci. Technol. 25 (2009) 1.
[4] Z.M. Sun, Y.C. Zhou, M.S. Li, Corros. Sci. 43 (2001) 1095.
[5] M.W. Barsoum, T. El-Raghy, L.U.J.T. Ogbuji, J. Electrochem. Soc. 144 (1997) 2508.
[6] H.B. Zhang, Y.C. Zhou, Y.W. Bao, J.Y. Wang, J. Mater. Res. 21 (2006) 402.
[7] H.B. Zhang, X. Wang, K.G. Nickel, Y.C. Zhou, Scr. Mater. 59 (2008) 746.
[8] R. Radakrishnan, J.J. Williams, M. Akinc, J. Alloys Compd. 285 (1999) 85.
[9] Y. Du, J.C. Schuster, H. Seifert, F. Aldinger, J. Am. Ceram. Soc. 83 (2000) 197.
[10] Z. Sun, Y. Zhou, J. Zhou, Philos. Mag. Lett. 80 (2000) 289.
[11] Z. Sun, J. Zhou, D. Music, R. Ahuja, J.M. Schneider, Scr. Mater. 54 (2006) 105.
[12] T. Okano, T. Yano, T. Iseki, Trans. Met. Soc. Jpn. 14A (1993) 597.
[13] C. Racault, F. Langlais, R. Naslain, J. Mater. Sci. 29 (1994) 3384.
[14] I.M. Low, Mater. Lett. 58 (2004) 927.
[15] I.M. Low, Z. Oo, K.E. Prince, J. Am. Ceram. Soc. 90 (2007) 2610.
[16] P. Eklund, C. Virojanadara, J. Emmerlich, L.I. Johansson, H. Högberg, L. Hultman, Phys. Rev. B 74 (2006) 045417.
[17] J. Emmerlich, D. Music, P. Eklund, O. Wilhemlsson, U. Jansson, J.M. Schneider, H. Högberg, L. Hultman, Acta Materialia 55 (2007) 1497.
[18] D.P. Riley, E.H. Kisi, J. Am. Ceram. Soc. 90 (2007) 2231.
[19] D. Music, D.P. Riley, J.M. Schneider, J. Eur. Ceram. Soc. 29 (2009) 773.
[20] M.W. Barsoum, T. El-Raghy, C.J. Rawn, W.D. Porter, H. Wang, E.A. Payzant, C.R. Hubbard, J. Phys. Chem. Sol. 60 (1999) 429.
[21] H.Z. Zhang, S.Q. Wang, Acta Materialia 55 (2007) 4645.
[22] Z. Wang, S. Tsukimoto, M. Saito, Y. Ikuhara, Phys. Rev. B 79 (2009) 045318.
[23] Z. Sun, R. Ahuja, Appl. Phys. Lett. 88 (2006) 161913.
[24] D. Music, Z. Sun, R. Ahuja, J.M. Schneider, Surf. Sci. 601 (2007) 896.
[25] J.P. Perdew, K. Burke, M. Ernzerhof, Phys. Rev. Lett. 77 (1996) 3865.
[26] J.M. Soler, E. Artacho, J.D. Gale, A. García, J. Junquera, P. Ordejón, D. Sánchez-Portal, J. Phys. Condens. Matter 14 (2002) 2745.
[27] S. Nosé, Mol. Phys. 52 (1984) 255.
[28] N.J. Lane, S.C. Vogel, M. Barsoum, Phys. Rev. B 82 (2010) 174109.
[29] Y. Waseda, K. Suzuki, Z. Phys. B 20 (1975) 339.